Modeling and validation of biogas consumption prediction in cook stove using a network approach

Authors contributions

This work was carried out in collaboration between all the authors. Author NB wrote the equations and the experimental protocol. IO wrote the first draft of the manuscript. Authors NB and IO implemented the program under Matlab. Authors DWNK and IO managed the analysis of the study and made corrections. Authors YMB and IO managed the bibliographic searches and checked the various calculations. The SD and SK checked the modeling and confirmed the discussion. All authors have read and approved the final manuscript.

Original Research Article

Abstract

This study seeks to propose a new model of hearth for the consumption of biogas produced by a biodigester of 4 m^{-3}. The cylindrical furnace is used to heat an empty pot for 3 hours. To do this, the system is subdivided into two sub-systems, the first of which is the flame, which then heats the bottom of the pot. The latter is the second hottest point. The developed network is composed of 8 isothermal points, interconnected by thermal resistances, each of which represents a particular type of heat transfer mode. The resolution of the system required 8 differential equations. The modeling allowed us to appreciate the temperatures governing the system. The experimental study proves an agreement with the model temperatures. Studies show that the optimal thickness and height of the hearth are respectively 12mm and 10 cm. The heat ide the internal air of the kettle is 220°C and the flame temperature is 900°C. The instantaneous efficiency of the firebox obtained is 65%. In addition, a validation with literature data to confirm this study, therefore its adoption will lead to reducing the consumption of biogas and therefore have a positive impact on the woodcut.

Keywords: Biogas, cook stove;validation;temperature; energy performance
2010 Mathematics Subject Classification: 53C25; 83C05; 57N16

1 Introduction

Households are the most dominant energy-consuming sector, accounting for around 80% of the country's total energy consumption (Vianello, 2017). According to the population census (Faso, 2022) shows that 76.4% of households in Burkina Faso use firewood and charcoal with a single hearth to cook food. Households using fuels (butane gas and biogas) represent 16.1% in country. The heavy reliance on the use of single cook stoves which have a relatively low conversion rate of biomass to energy is one of the factors contributing to the over-consumption of biomass resulting in an increased rate of forest degradation. Butane gas is experiencing disruptions in distribution, which are hampering its adoption by households. Given this situation, researching technologies to improve the conversion of biomass to energy in even a small country can have an overall impact on the economy of available fuel. It is in this sense that the government of Burkina Faso has set up the National Biodigester Program to offer an alternative to fuelwood(Whitman et al., 2011). Thus, optimizing the energy consumption of the household will allow the acceptance of the biodigester technology in a household which can lead to the adoption of biodigesters is the desired goal(Ceballos et al. 2015). This study was motivated by the need to assess stove energy efficiency. The stove prototype is cylindrical in shape with a burner containing a 3.5mm nozzle fed with 60% methane biogas. The study focuses on modeling under MATLAB $R2021b$® by the thermal network approach and experimentation. At the end we will have the optimal dimensions of an energy efficient cook stove compared to existing.

Abbreviations		
A1...A8	surface of the cook stvove	m^2
PCI	Power Calorific Value	$kJ.L^{-1}$
D	biogas flow	$L.s^{-1}$
Cd	coefficent de pertes de charge	J^{-1}
Cp	Chaleur spefique	W(mK)
m	Mass	kg
λ	Thermal conductivity	$(W.m^{-2}.K)$
p	Density	kg.m3
Ta...Th	Temprature	°C,K
β	coefficient of expansion	$°C^{-1}$
Gr	Nombre de grasoft	Without unit
Nu	Number of nussselt	Without unit
F	Form Factor	Sans unite
Ra	Number of Raleigh	Without unit
Pr	Number of Prandtl	Without unit
p	Pression	atm
Q	Quantity of energy	J
η	energy efficiency	%

2 Materials and Methods

2.1 Presentation of the model

The system is subdivided into two subsystems $\{a, b, c, d, k,\ h\}$ et $\{d, e, f, g,\ h\}$ The way it works is that the heat source point exchanges with points a, b, c, d, h, and k. The greatest exchange is with point d which will later become the second hottest point. This last point will exchange vice versa with the points e, f, g, and the ambient medium k. Point d acts as a bridge between the two subsystems. Conduction was studied between h and a, considering the strong heat coming from the burner at point a and the doubled thickness of 14 mm between a and h. The search for the temperature of the internal air of the kettle is the objective of the heating. The physical model and the circuit allowing the discretization of the equations are represented in 1a and 1b.

Simplifying assumptions

Assumptions are adopted to simplify the modelling.

- The airflow is even in the burner
- The heat flux and temperature of each component are uniform at each time step
- The volume of air in the pot is constant
- The temperature of the outdoor air and the fireplace is uniform and the same as that of the floor
- Heat loss around fireplace does not affect room temperature
- No mass transfer is considered
- The derivative is a function of the time in the discretization.

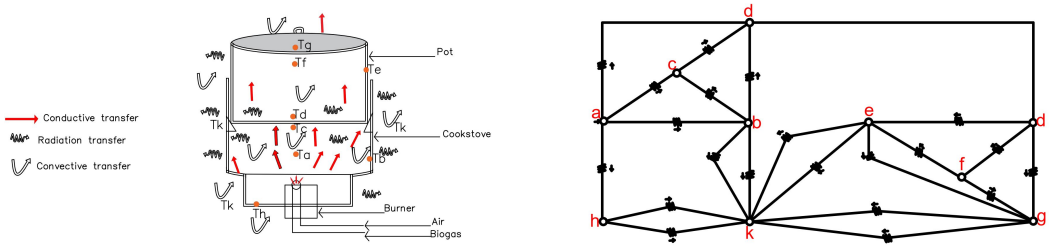

(a) Physical model (b) temperature network

Figure 1: Study method and diagram of the equivalent circuit of the discretization of the hot spots

2.2 Stove presentation

The pot is constructed from 14mm thick iron and the pot is recycled aluminum. The height of the hearth is 30 cm from the ground. With a radius of 15 cm and the height of the combustion chamber is 10 cm, playing the role of the tunnel that can lead the hot gases to the pot. It is designed on two levels, the first is the combustion chamber with a diameter of 10 cm and the second allows to house the pot with a thickness of 2 cm. A 13cm radius pot is designed to fit snugly into the fire pit to prevent leaks. The pot has a lid of the same material as the pot with a radius of 14 cm. The cover covers it during the test to fit without any air intake gap. The biogas arrives at the chimney with a 3.5 mm diameter burner through a pipe from the biodigester. 09 thermocouples are used to take the temperatures which are recorded in the mini data logger; The hearth device is shown in figure 2a and that of the entire device from 2b for testing.

Fuel quantity calculation

The amount of fuel is obtained by the equation of Bernoulli's theorem in fluids (Kurchania et al., 2010) presented in 2.1. With D, the diameter of the burner (mm), p the pressure (kPa) and the density of the biogas ($kg.m^{-3}$). The discharge coefficient is 0.9 is obtained from the Bernoulli diagram. The loss coefficient is introduced to account for all inefficiencies of the included flow tube effect $\in [0; 1]$ (Petro et al., 2020)

$$q_{comb} = Q_{biogas}.PCI = 0,036.Cd.D^2.\sqrt{\frac{p}{\rho}}.PCI \tag{2.1}$$

Numerical study of the thermal efficiency of the fireplace

The instantaneous efficiency is determined by considering the quotient of all the energies arriving on the kettle as useful energy by the energy of combustion. The energy received

(a) Study cook Stove (b) Experimentation with the fireplace

Figure 2: Type of stove and the complete experimentation device

by the pot is given by:

$$Qu = \frac{\left[\begin{array}{l} m_{pot}cp_{pot}(T_d - T_0) + m_{pot}cp_{pot}(T_e - T_0) + \\ +m_{air2}cpair_2(T_f - T_0) + m_{\text{cover}}cp_{\text{cover}}(T_g - T_0) \end{array}\right]}{Times} \tag{2.2}$$

$T_0)$ is the value of the initial temperature which is at the same time the ambient value. The yield is now given by:

$$\eta = \frac{Qu}{q_{comb}}.100 \tag{2.3}$$

This function is entered into the program with the same time step as the temperature calculations.

Thermal exchange at the flame

The conservation equation of energy from burning biogas to heat the combustion chamber is:

$$m_{comb}\text{Cp}_{comb}\frac{dT_a}{dt} = \left[\begin{array}{l} A_1F_{12}.\sigma({T_b}^d - T_a^4) + h_1A_1.(T_c - T_a) + \\ +A_1F_{12}.\sigma({T_d}^4 - T_a^4) + U_{1-8}A_1.aa(T_d - T_1^4) + q_{comb} \end{array}\right] \tag{2.4}$$

The heat produced by the exothermic combustion of the gas is around 900C, of which the specific heat of the air mixing with the biogas is 0.9536 kJ/kg/C (Augustin et al., 2022). Thus, the equation of this quantity of energy at the level of the burner was calculated 2.1

Heat exchange at the hearth wall

The temperature of the wall of the furnace is close to the flame and calculated according in 2.5.

$$m_{w1}\mathrm{Cp}_{w1}\frac{dT_b}{dt} = \left[\begin{array}{l} A_2F_{21}\sigma({T_a}^4 - T_b^4) + h_1A_2(T_c - T_b) + A_3({T_k}^4 - T_b^4) + \\ +A_2F_{24}\sigma({T_d}^4 - T_b^4) + h_3A_3(T_k - T_b) \end{array} \right] \tag{2.5}$$

Heat exchange at the combustion chamber

the heat balance in the combustion chamber is described in the equation 2.6.

$$m_{air,1}\mathrm{Cp}_{air,1}\frac{dT_c}{dt} = \left[\begin{array}{l} h_1A_1(T_a - T_c) + h_1A_2(T_a - T_c) + \\ +h_1A_4(T_a - T_c) \end{array} \right] \tag{2.6}$$

Heat exchange at the base of the kettle

The base of the firebox is the part in direct contact with the flame and the equation is presented in 2.7

$$m_{pot}\mathrm{Cp}_{pot}\frac{dT_d}{dt} = \left[\begin{array}{l} A_2F_{41}\sigma.({T_a}^4 - T_d^4) + h_1.A_4(T_c - T_d) + \\ +A_2F_{42}\sigma.({T_b}^4 - T_d^4) + A_5F_{45}\sigma.({T_e}^4 - T_d^4) + \\ +h_2A_5.(T_f - T_b) + A_5F_{47}\sigma.({T_g}^4 - T_d^4) \end{array} \right] \tag{2.7}$$

Thermal exchanges at the level of the pot thickness

The energy balance between the walls of the pot and the other points is presented by 2.8.

$$m_{pot}\mathrm{Cp}_{pot}\frac{dT_e}{dt} = \left[\begin{array}{l} A_6F_{54}\sigma({T_d}^4 - T_e^4) + h_2A_6(T_f - T_e) + \\ +A_6F_{57}\sigma({T_g}^4 - T_e^4) + A_7F\sigma({T_k}^4 - T_e^4) + \\ +h_3A_7(T_k - T_e) \end{array} \right] \tag{2.8}$$

Heat exchange inside the pot

The pot is empty, the air is heated whose energy balance equation is 2.9.

$$m_{air,2}\mathrm{Cp}_{air,2}\frac{dT_f}{dt} = \left[\begin{array}{l} h_2A_5(T_d - T_f) + h_2A_2(T_e - T_f) + \\ +h_2A_8(T_g - T_f) \end{array} \right] \tag{2.9}$$

Heat exchange at the pot lid

The heat balance on the lid of the pot is given in 2.10.

$$m_{\text{cover}}\text{Cp}_{\text{cover}}\frac{dT_g}{dt} = \left[\begin{array}{l} h_2A_8(T_f - T_g) + A_8F_{75}\sigma({T_e}^4 - T_g^4) + \\ +A_9F\sigma({T_k}^4 - T_g^4) + A_8F_{74}\sigma * ({T_d}^4 - T_g^4) + h_3A_9(T_k - T_g) \end{array} \right] \tag{2.10}$$

Heat exchange at the cook stove base

The lining of the base of the fireplace reduces the heat transfer from the burner to the bottom of the fireplace. The energy balance at the bottom of the fireplace, i.e. the most insulated part of the fireplace, is presented in 2.11.

$$\text{m}_{w,2}\text{Cp}_{w,2}\frac{dT_h}{dt} = \left[\begin{array}{l} h_2A_8(T_k - T_h) \\ +A_8F\sigma({T_k}^4 - T_h^4) \end{array} \right] \tag{2.11}$$

$$Cp\_air_1 = (0.9362 + 0.0002 * (Ta\,(i))) \tag{2.12}$$

Determining the constants

The constants follow the three modes of heat transfer. The conduction considered at the bottom of the focus is given by 2.13.

$$U_{1-8} = \frac{K_{foyer}}{e_{base}} \tag{2.13}$$

With K_{foyer},the conductivity of iron and e_{base} the thickness of the focus.
The form factor to calculate the radiation coefficient between two points i and j is given by 2.14.

$$F_{ij}eq = \frac{1}{\frac{1}{\varepsilon_i} - 1 + \frac{1}{F_{ij}} + \frac{S_i}{S_j}\left(\frac{1}{\varepsilon_i} - 1\right)} \tag{2.14}$$

F_{ij} the shape factor between the surface of S_i and S_j; ε_i, ε_j are the permissivities of the surfaces. The focus is a black body so ε is 1 and that of the pot (aluminum) is 0.8. After reduction, the radiative exchange coefficient between two bridges becomes 2.15

$$hr_{i-j} = \sigma\varepsilon({T_i}^2 + {T_j}^2) * (T_i + T_j) \tag{2.15}$$

The interior of the combustion chamber having the shape of a tube whose $D < L$ is in natural convection. The Nusselt number is given by the relation 2.16

$$Nu_1 = 0,023.Re^{0,8}(1 + (D/L))^{(0.7)}.0,685^{(1/3)} \tag{2.16}$$

The interior of the empty pot and the surrounding medium are in natural convection (Zube et al., 2021) so the Nusseelt number is given by the relation 2.17.

$$Nu_2 = 0,54(Gr.\,\text{Pr})^{(0.25)} \tag{2.17}$$

The rest of the constants, namely the number of Grassoft Gr , prandlt, thermal expansion β and the coeffiction h of convection are given in 2.19 and **??**

$$Gr = \frac{g.\beta.T.L^3.\rho^2}{\mu^2}; Pr = \frac{\mu.Cp}{k} \tag{2.18}$$

$$\beta = 1./T; h = \frac{Nu.k}{L} \tag{2.19}$$

2.3 Model validation

The numerical validation consisted in retrieving the author's numerical data and finding a polynomial equation describing these data(Tampango et al., 2011) according to 2.20.

$$y = a_n x^n + a_{n-1} x^{n-1} + a_1 x^1 + ... + a_0 \tag{2.20}$$

With a the coefficients and n the degree of the polynomial. This polynomial is implemented under Matlab in order to determine the errors committed on the results with the static formula RMSE (Root Mean Square Eroor)(Guermoui et al., 2022) present in 2.21

$$RMSE = \sqrt{\frac{1}{N}\sum_{1}^{N}\left(y_{\exp}(t_i) - y_{sim}(t_i,\theta)\right)^2} \tag{2.21}$$

yexp are the collected measurements, , ysim are the data predicted by the model, θ represents the parameters to be determined and N is the number of measurements.

3 Numerical resolution procedure

Partial derivative equations are reduced to a system of algebraic equations. The dimensions of the hearth are considered in our calculation code. We proceed to read the coefficients These elements allow us to calculate the first four terms (k1, k2, k3, and k4) from **RUNGE KUTTA** to $T(i)$. Then the temperature value $T(i+1)$ is determined explicitly and so on the program runs over a multiple number of steps. A total of eight temperatures are to be determined with a **for** loop until the time of $n-1$ before displaying the results. When a solution of the temperatures foresees unsatisfactory results in a region, a modification of the time step is made. With several attempts, a time step of 0.1s is retained.

4 Results and Discussion

4.1 presentation of results

The figures below show the evolution of all 08 experimental and simulation temperatures as a function of time.

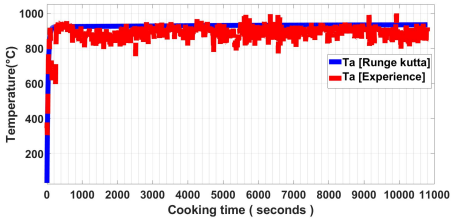

(a) Flame

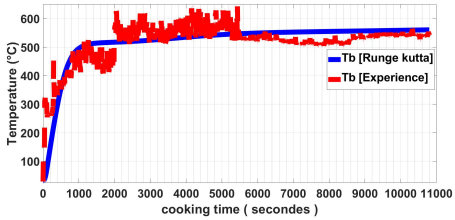

(b) cooker wall

Figure 3: Temperatures of the and the thickness of the hearth

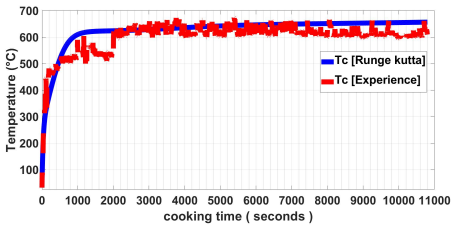

(a) Combustion chamber

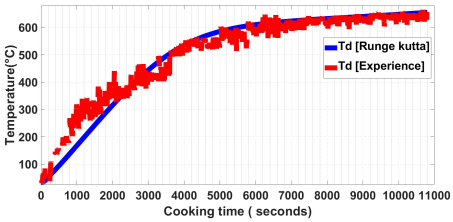

(b) pot base wall

Figure 4: Temperatures of the combustion chamber and the base of the pot

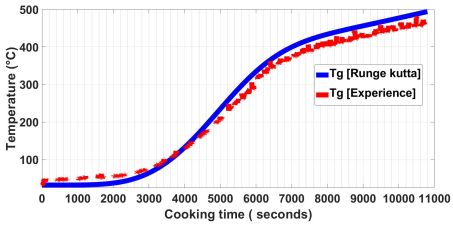

(a) lid

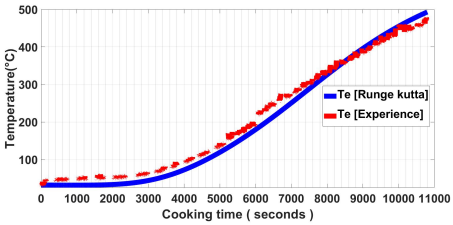

(b) vertical wall of the pot

Figure 5: Temperatures of the lid and the base of the pot

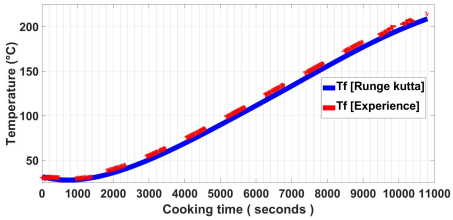

(a) internal pot temperature

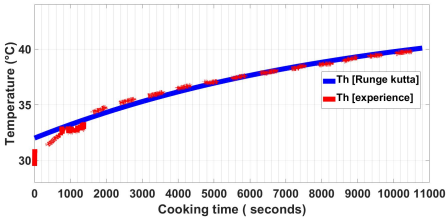

(b) base wall of the fireplace

Figure 6: Internal air temperatures of the pot and the base of the fireplace

The presented flame temperatures Ta 3a reach their maximum at 900 °C at t= 500 seconds and remain stable. This good result at the quality of the biogas raised 60% of CH_4 according to the work of Jiang (Jiang et al., 2018) whose PCI = $37.78kJ.L^{-1}$. The 3.5 mm nozzle burner factor achieves this result by helping to obtain a good air-fuel mixture (Devi et al., 2019). The simulated and experimental temperature Tb in figure 3b obtain values of 500 °C and 465 °C respectively. This result

is favored by the thermal inertia created by the burner thickness of 14mm (Powell et al., 2021). Also, the 13 cm diameter of the fireplace allows the flame temperature to touch the walls, increasing its temperature. The figures 4a of the combustion chamber temperatures Tc are found at t=10 min at T= 600 °C. The characteristics of the fireplace, namely its thickness, diameter and height, lead to this result. The height of 10 cm and diameter of 13 cm gives a reduced volume to be heated. Also the cylindrical shape fits well with the pot avoiding the renewal of air in the room. The curves in the figure 4b show a slow evolution to reach values to reach its maximum of Td =500 °Cat t = 500s. We find that the heat transfers in the enclosure are influenced by the increase in the heat flux of the burner. Thus, the hot air from the chamber is directed directly to the base of this pot keeping its temperature high at 500C. Moreover, we see that the temperature of the base of the pot presented in the figure 2.7 is not different from that of the flame and this explains a good transfer of heat towards the pot. The temperature curves of the air inside the pot reached a maximum of 220°C. Nevertheless, we notice a difference between this temperature and that of 900°C. This is due either to losses related to the characteristics of the pot (thickness = 2mm, aluminium) or to the continuous renewal of the air within the pot. Looking for a steel pot would yield better results. This result is sufficient to cook any type of meal according to the work of bastista (Batista et al., 2019). Bagaya et al (Bagaya et al., 2021) on hotplates found a temperature of 408.2 °C and sufficient to prepare any type of food.The curves in the figures 5a and 5b show respectively the temperatures of the lid and the thickness of the pot. We observe temperatures of 400°C. These results also represent losses dissipated by the pot. This result shows that the pot has a low thermal inertia (Huang et al., 2009). The figures 6b show the temperatures of the hearth base corresponding to the losses due to the wall of the hearth. The temperature of the losses Th is around 60 °C which is a progress and similar to the work of SagouongSagouong and 2018 whose result of the parietal loss Th is 80 °C. This result that the thickness of 14mm doubled at the base of the hearth made it possible to preserve the temperature within the combustion chamber. This good result makes it possible to reduce the loss of heat which is the problem of open hearths (Gandigude and Nagarhalli, 2018). The experimental temperatures give a good look with the simulated temperatures showing a good prediction of the not good prediction of the reduction of heat losses.

4.2 Study validation

The figure 7a represents the study of the hottest temperature validation of the hearth between our study and that of sagnoug. Both studies used the RUNGE KUTTA method implemented in Matlab. The temperature of the sagnoug flame is 750K and 802K for our study at time t = 150s. This observed difference of the two flames is justified by the heat source of the two studies, i.e. the nature of the hearth according to the work of Kausley et al (Kausley and Pandit 2010). Our heat source is biogas fuel and that of Sagnoug is coal. This delay e, ignition leads to low heat production without forgetting the PCI of coal lower than the PCI of biogas (Russell et al. 2013). Also our black colored steel hearth reduces losses compared to the aluminum author's hearth. The two curves stabilize around 800K after 400 seconds of simulation. The comparison of the calculation error between the two studies is 0.4 K at the end of time t = 800 seconds. We can say that our simulated curve admits the same pace as that obtained by Sagouong (Sagouong, Tchuen, 2018) proving the

effectiveness of the RUNGE KUTTA model. The curves in the figure 7b show the efficiency of our study and that of Khaushik in a time of 10800 seconds. At t= 0s the η are 0%, 15% respectively for our study and that of the author. After a time t = 6000s the performance of our study is 50% and that of Khaushik (Kaushik, 2019) is 49%. It is from this time of 600 seconds that an error deviation (RMSE) of 4% is created with our study. The author's study is superior to our study and this is due to his CFD digital model used, i.e. the ceramic which is the protective insulation of the fireplace. Sowgath showed that CFD is a somewhat simplified structure for analyzing temperature profiles (Sowgath et al. 2015) The experimental and simulation figures at the level of the flame show a variation of 900 °C at 850 °C at t=2000s. After this time the two are in agreement a with a difference of 3%. For the other experiments, the greatest deviation of 5.75% is observed at the level of temperature (Tc). These differences are due to the phenomenon of the wind sometimes creating a vortex effect in the combustion chamber during the experiment and the renewal of air in the pot. On the whole, the values predicted by the model are acceptable and provide a solution for the manufacture of stoves.

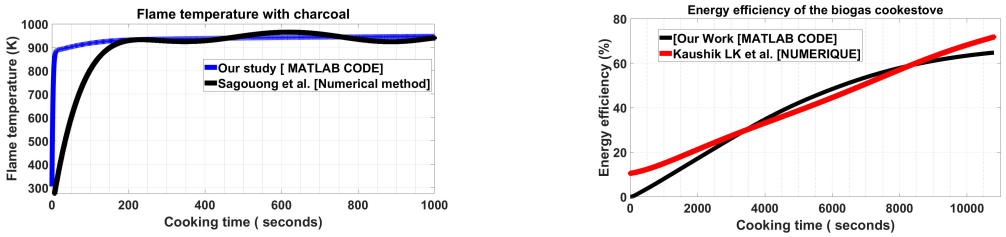

(a) Flame (b) combustion chamber

Figure 7: Flame temperature validation with the numerical model of sagnoug et al and thermal efficiency validation of the firebox with the Khaushik model LK et al

4.3 Influence of focus thickness

The figure 8b shows the influence of the thickness on the energy loss by the base of cook stove called the insulation. The figure 8a presents the thermal efficiency. For a thickness e=14 mm, the efficiency is approximately 65 % and the base temperature is 45 °C.

In general, the increase in thickness leads to a gain in thermal efficiency and a reduction in energy losses to the environment. On the other hand, a thickness of less than 10 mm results in a yield of 25 % and a loss of up to 100 °C. This is because the thickness allows control of the thermal inertia of the cook stove. The

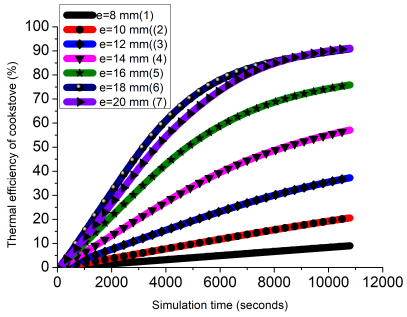

(a) Thermal efficiency

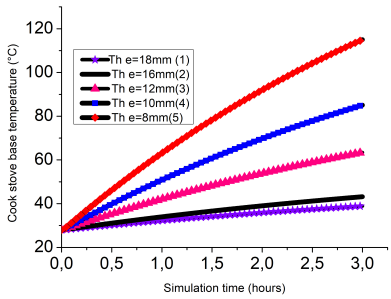

(b) Insulation temperature

Figure 8: Internal air temperatures of the pot and the base of the fireplace

conduction studied at point (h) shows that for a thickness of 8 mm the temperature Th is at 115 °C in 03h. This can also be explained by the fact that the heat transfers by conduction between the center of the hearth enclosure and the wall of the hearth becomes weak if the thickness of the hearth is high and strong if the thickness becomes more and more. strong. For a thickness e= 18 mm the energy efficiency reaches 90 % which means a quantity of energy is sent to the pot.

An increase in the height of the combustion chamber, the flame does not reach the bottom of the pot. This results in a large combustion chamber surface area, which reduces wall temperatures. Therefore, the height leads to a decrease in thermal efficiency. With a height H= 14 cm the $\eta = 40\backslash\%$, H= 10 cm $\eta = 65\backslash\%$ and H=10 $\eta = 70\backslash\%$ the temperature. This shows the lower the height, the closer the pot is to the flame, therefore a high thermal gradient (Ta=900°C) is recovered by the pot. The optimal height is H= 9cm beyond that, there is no longer any gain illustrated in the curve 9b. This means from 9cm all the energy detectable by the pot is reached.

The optimal thickness is e=18mm beyond which no energy is observed as shown in the figure 8a.

4.4 Influence of combustion chamber height

The figures **??** show the evolution of the temperature in the kettle and the efficiency as a function of time.

5 CONCLUSION

This work, the objective of which was to propose a prototype of an energy efficient biogas stove, has yielded results. The fireplace studied numerically under MATLAB $R2021b$® gave results in line with the experiment. The biogas flame reached a temperature of 900 °C and the combustion chamber around 600 °C. The temperature of the interior air of the pot reached is 220 °C which can cook a meal according to the work of Shen (Shen et al., 2017). The instantaneous thermal efficiency of the fireplace is 65%. It appears from this study that the optimal height of the combustion

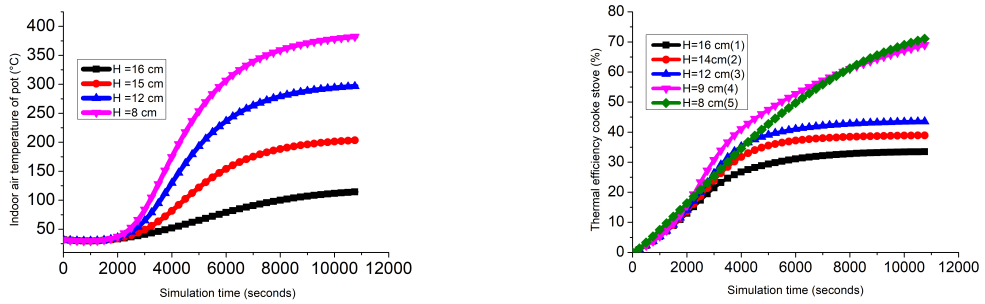

(a) within the pot

(b) Thermal efficiency

Figure 9: Impact of chamber height on internal pot temperature and energy efficiency

chamber is 10 cm and the optimal thickness is 18 mm. Numerical validation with the literature (Kaushik, 2019) gives agreement with a maximum car of 6%. This result is better compared to Bagaya's study (Bagaya et al., 2021) on the biogas stove, for which $\eta = 55\backslash\%$, therefore acceptable according to the literature (Grimm, 2014). However, the energy performance of the home will drop in a busy kitchen, but its adoption by cooking stove is already an important step in reducing wood cutting in Burkina Faso.

Acknowledgment

This article follows on from research supported by the National Biodigesters Program of Burkina Faso (PNB-BF) and International Scientific Program (ISP),University of Uppsala, Sweden through project BUFO1 funding. Also the Embassy of France in Burkina Faso is recognized for its financing of Bagaya Noufou's research stay in Paris Saclay University.

COMPETING INTERESTS

Authors have declared that no competing interests exist.

References

Augustin, L. M., Vertomene, S. T., Bernard, N. N., Sadiki, A., and Haddy, M. K. (2022). A New Perspective on Cooking Stove Loss Coefficient Assessment by Means of the Second Law Analysis. 127.

Bagaya, N., Ouedraogo, I., Wind, D., Koumbem, N., Sandwidi, G. W., and Kieno, F. P. (2021). Energy Performance Analysis of B1-3 . 5mm Burner Model of Fasobio-15 Biodigester Biogas Cookstoves. 25(7), 1121. https://doi.org/10.9734/PSIJ/2021/v25i730268

Batista, C. de S., dos Santos, J. P., Dittgen, C. L., Colussi, R., Bassinello, P. Z., Elias, M. C., and Vanier, N. L. (2019). Impact of cooking temperature on the quality of quick cooking brown rice. Food Chemistry, 286(January), 98105. https://doi.org/10.1016/j.foodchem.2019.01.187

Ceballos, Gerardo et al. 2015. Accelerated Modern Human-Induced Species Losses: Entering the Sixth Mass Accelerated Modern Human Induced Species Losses: Entering the Sixth Mass Extinction. (June).

Chakchak, Sawssen and Hidouri, Ammar and Zaidaoui, Hajar and Chrigui, Mouldi and Boushaki, Toufik (2021).Experimental and numerical study of swirling diffusion flame provided by a coaxial burner: Effect of inlet velocity ratio, journal MDPI =Fluids, volume=6,pages=159,

Devi, S., Sahoo, N., and Muthukumar, P. (2019). Combustion of biogas in Porous Radiant Burner: Low emission combustion. Energy Procedia, 158, 11161121. https://doi.org/10.1016/j.egypro.2019.01.276

Faso, B. (2022). Cinquime Recensement Gnral de la Population et de lHabitation du Burkina Faso.

Guermoui, M., Abdelaziz, R., Gairaa, K., Djemoui, L., and Benkaciali, S. (2022). New temperature-based predicting model for global solar radiation using support vector regression. International Journal of Ambient Energy, 43(1), 13971407. https://doi.org/10.1080/01430750.2019.1708792

Grimm, M. (2014). Impact Evaluation of Improved Stove Use among Dolo-beer Breweries in Burkina Faso FAFASO. July 2013, 131.

Huang, Y., Risha, G. A., Yang, V., and Yetter, R. A. (2009). Effect of particle size on combustion of aluminum particle dust in air. Combustion and Flame, 156(1), 513. https://doi.org/10.1016/j.combustflame.2008.07.018

Jiang, X., Mira, D., and Cluff, D. L. (2018). The combustion mitigation of methane as a non-CO2 greenhouse gas. Progress in Energy and Combustion Science, 66, 176199. https://doi.org/10.1016/j.pecs.2016.06.002

Kaushik, L. K. (2019). Performance and Feasibility Assessment of Porous Radiant Burner Aided Cook-stoves for LPG , Biogas and Waste Cooking Oil Fuels Doctor of Philosophy by Department of Mechanical Engineering Indian Institute of Technology Guwahati Department of Mechanical En.

Saber, Meryem et al. 2021. Enhancement of Organic Household Waste Anaerobic Digestion Performances in a Thermophilic Pilot Digester. Biomass and Bioenergy 144(July 2020): 105933. https://doi.org/10.1016/j.biombioe.2020.105933.

Kausley, Shankar B, and Aniruddha B Pandit. 2010. Modelling of Solid Fuel Stoves. Fuel 89(3): 78291. http://dx.doi.org/10.1016/j.fuel.2009.09.019.

Kurchania, A-K, Panwar, N. L., and Pagar, S. D. (2010). International Journal of Sustainable Energy Design and performance evaluation of biogas stove for community cooking application Design and performance evaluation of biogas stove for community cooking application. International Journal of Sustainable Energy, 29(2), 116123. http://www.tandfonline.com/action /journalInformation?journalCode=gsol20

Gandigude, A. and Nagarhalli, M. (2018). ScienceDirect Simulation of Rocket Cook-Stove Geometrical Aspect for its Performance Improvement. Materials Today: Proceedings, 5(2), 39033908. https://doi.org/10.1016/j.matpr.2017.11.645

Petrol, L. M., Machunda, R., Tumbo, S., and Kivevele, T. (2020). Theoretical and Experimental Performance Analysis of a Novel Domestic Biogas Burner. 2020.

Powell, T., ODonnell, R., Hoffman, M., Filipi, Z., Jordan, E. H., Kumar, R., and Killingsworth, N. J. (2021). Experimental investigation of the relationship between thermal barrier coating structured porosity and homogeneous charge compression ignition engine combustion. International Journal of Engine Research, 22(1), 88108. https://doi.org/10.1177/1468087419843752

Russell, A et al. 2013. Using Forests to Enhance Resilience to Climate Change: The Case of the Wood-Energy Sector in Burkina Faso.

Tampango, Y., Potier-ferry, M., Koutsawa, Y., Tampango, Y., Potier-ferry, M., and Koutsawa, Y. (2011). Une mthode sans maillage base sur la rsolution de l EDP par sries de Taylor To cite this version: HAL Id: hal-00592826.

Sagouong, J. M., and Tchuen, G. (2018). Mathematical modelling of traditional stoves using the Thermal Network Approach. April. https://doi.org/10.14445/22315381/IJETT-V58P201

Shen, G., Hays, M. D., Smith, K. R., Williams, C., Faircloth, J. W., and Jetter, J. J. (2017). Evaluating the Performance of Household Liquefied Petroleum Gas Cookstoves Evaluating the Performance of Household Liquefied Petroleum Gas Cookstoves. https://doi.org/10.1021/acs.est.7b05155

Sowgath, Tanvir, Mominur Rahman, Sabbir Ahmed Nomany, and Nazmus Sakib. 2015. CFD Study of Biomass Cooking Stove Using Autodesk Simulation CFD to Improve Energy Efficiency and Emission Characteristics. 45: 125560.

Vianello, M. (2017). The Energy Situation in Goudoubo Refugee Camp, Burkina Faso. May.

Whitman, T., Nicholson, C. F., Torres, D., and Lehmann, J. (2011). Climate change impact of biochar cook stoves in western kenyan farm households: System dynamics model analysis. Environmental Science and Technology, 45(8), 36873694. https://doi.org/10.1021/es103301k

Zube, N. G., Zhang, X., Li, T., Le, T., Li, C., Guerlet, S., and Tan, X. (2021). Radiative-dynamical Simulation of Jupiters Stratosphere and Upper Troposphere. The Astrophysical Journal, 921(2), 174. https://doi.org/10.3847/1538-4357/ac1e95